11

Molecular Dynamics Studies of the Process of Crystallization and Growth of Gas Hydrates in a Strongly Supercooled Two-Phase „Methane–Water System“

© R.M. Khusnutdinoff [1,2], R.R. Khairullina [1], M.B. Yunusov [1]

[1] Kazan Federal University,
Kazan, Russia
[2] Udmurt Federal Research Center, Ural Branch Russian Academy of Sciences,
Izhevsk, Russia

E-mail: khrm@mail.ru

Received November 8, 2022
Revised November 8, 2022
Accepted November 12, 2022

The processes of nucleation and growth of methane hydrate in a highly supercooled two-phase „methane–water“ system obtained using various cooling protocols are considered. It has been shown that, at sufficiently high cooling rates, crystalline forms of methane hydrate can still form in the system. It was found that, at a cooling rate of $\gamma = 1.0$ K/ps, the process of nucleation and growth of gas hydrate was observed in all independent molecular dynamics iterations, while at a cooling rate of $\gamma = 10.0$ K/ps, no nucleation event was observed in $\sim 26.7\%$ of numerical experiments. It was found that with an increase in the cooling rate of the system, an increase in the average time scale of nucleation τ_c and a decrease in the critical size of the nucleus n_c are observed. It is shown that at a sufficiently deep level of supercooling of the system, the scenario of homogeneous crystalline nucleation is realized at the initial stage of the phase transition.

Keywords: molecular dynamics, crystallization, methane hydrate.

DOI: 10.21883/PSS.2023.02.55420.522

1. Introduction

Identification of nucleation processes in „host–guest“ type molecular complexes is one of the essential challenges of the condensed matter physics. The examples of such systems include natural hydrates — gas hydrates [1–4]. They consist of gas molecules (guest molecules) enclosed in the cavities of three-dimensional lattices formed by water molecules — water clathrate cages (host cages) [5]. Natural hydrates are one of the gas existence forms in the Earth's interior and are among promising hydrocarbon gas sources [6]. Gas hydrates are formed at low temperatures and high pressures, and occur naturally in permafrost regions and on continental shelf bottom. The focus on the investigation of these compounds is explained by the prospect of wide industrial and power application [6,7]. Since gas hydrate density is close to the density of liquified gases, extensive utilization of gas hydrates is expected for gas transport and storage. Moreover, the ability of gas hydrates, while growing, to displace ions from a crystalline lattice may be used for water treatment. Natural gas hydrates, in particular, the most common methane hydrate play an important role in oil and gas industry for two reasons. First, the natural gas hydrate reserves are estimated to be much higher than reserves of all other types of hydrocarbons in energy equivalent. Second, temperature and pressure conditions on gas and oil pipeline walls facilitate formation of natural gas hydrates which are built on pipe walls resulting in pipe capacity reduction and blocking. Natural gas hydrates can be also treated as possible climate change factor because sudden methane hydrate dissociation on the ocean bottom can result in methane outburst to atmosphere and, together with high greenhouse activity, contribute to global warming [8,9].

Thus, identification of nucleation processes in molecular complexes such as „host–guest“ is still one of the most important remaining challenges of phase transition and critical event physics. Large-scale molecular dynamics study of gas hydrate crystallization and growth processes in highly overcooled two-phase „methane–water“ system are discussed herein.

2. Modelling details

Methane hydrate crystallization and growth in highly overcooled two-phase „methane–water“ system was simulated in LAMMPS [10] package. Initial system configuration was composed of 64 $(4 \times 4 \times 4)$ sI-methane hydrate lattice cells consisting of 2944 water molecules and 512 methane molecules (see Figure 1). Molecule interaction was enabled by a coarse-grained interparticle interaction model that has higher computational efficiency than full-atom models [11]. Nose–Hoover thermostat and barostat with $\tau_T = 0.1$ and $\tau_p = 1.0$ ps were used for modelling in NpT-assembly. Molecule motion equations were integrated using the Verlet algorithm in a rate form with time interval

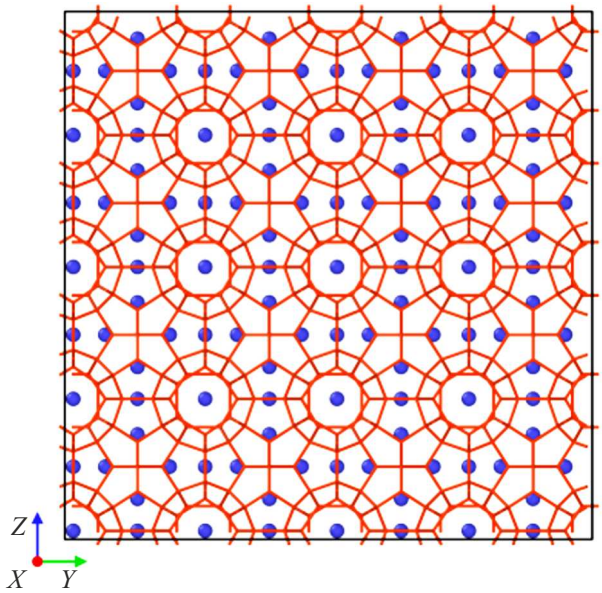

Figure 1. Hydrogen bond topology in the initial modelling cell. Bonds are shown by lines, methane molecules are shown by circles, water molecules are not shown.

$\tau^* = 10.0$ ($\tau = 12$ fs). Periodic boundary conditions were superimposed in all three directions.

The first modelling stage involved melting of the methane hydrate crystalline lattice at $T = 425$ K and $p = 500$ atm until the initial crystalline structure disappears completely and two-phase liquid „methane–water" system is formed. At the second stage, the produced system was cooled down to $T = 210$ K. The system was cooled down at rates $\gamma = 1.0$ and 10.0 K/ps. At the next stage, curing of this system and methane hydrate formation process occurred during 50 s. For statistic processing of modelling results at each cooling rate, 30 independent numerical experiments were carried out.

3. Findings and discussion

For clathrate structure identification, CHILL+ cluster analysis method was used[13] which was based on the calculation of the correlation function of local orientational order parameters [14,15]:

$$c(i,j) = \frac{q_l(j)\cdot q_l(j)}{|q_l(i)|\,|q_l(j)|} = \frac{\sum\limits_{m=-l}^{l} q_{lm}(i)q^*_{lm}(j)}{\left(\sum\limits_{m=-l}^{l} q_{lm}(j)q^*_{lm}(j)\right)^{1/2}\left(\sum\limits_{m=-l}^{l} q_{lm}(j)q^*_{lm}(j)\right)^{1/2}}. \quad (1)$$

Here, $q_l(i)$ is the l-order local orientation parameter for the i-th water molecule which is a vector with $2l+1$ complex components.

$$q_{lm}(i) = \frac{1}{4}\sum_{j=1}^{4} Y_{lm}(Q_{ij}, \varphi_{ij}), \quad (2)$$

where $Y_{lm}(\theta_{ij}, \varphi_{ij})$ — are spherical harmonics, θ_{ij} and φ_{ij} define the polar and azimuth angles, respectively, formed by radius vector $\mathbf{r}_{ij}$ in the spherical coordinate system.

Figure 2 shows the cluster analysis for highly overcooled two-phase „methane–water" system at $T = 210$ K and $p = 500$ atm with quick system cooldown at rate $\gamma = 10.0$ K/ps. Hydrate phase was identified using CHILL+ algorithm with the appropriate hydrogen bonds highlighted in orange. Blue circles are methane molecules, white circles are water molecules which are not in the hydrate phase.

The Figure shows that crystalline forms of methane hydrate occur during deep overcooling. Moreover, the hydrate nucleation and growth process starts already at early stages (about several nanoseconds). The methane

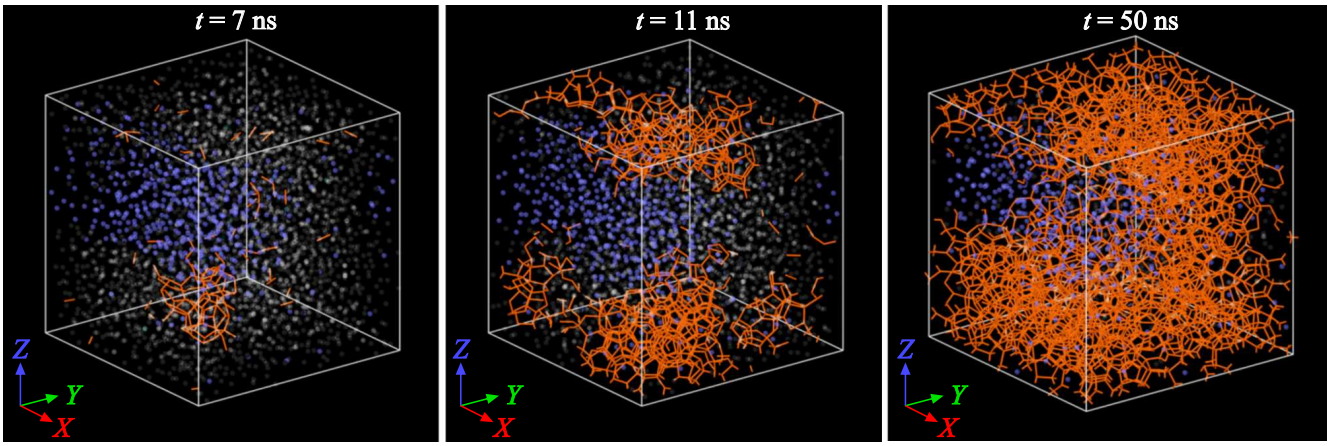

Figure 2. Methane hydrate crystal nucleation and growth from overcooled two-phase liquid „methane–water" at $T = 210$ K and $p = 500$ atm. System cooling rate is $\gamma = 10.0$ K/ps. Hydrate phase was identified using CHILL+ algorithm with the appropriate hydrogen bonds highlighted in orange. Blue circles are methane molecules, white circles are water molecules which are not in the hydrate phase.

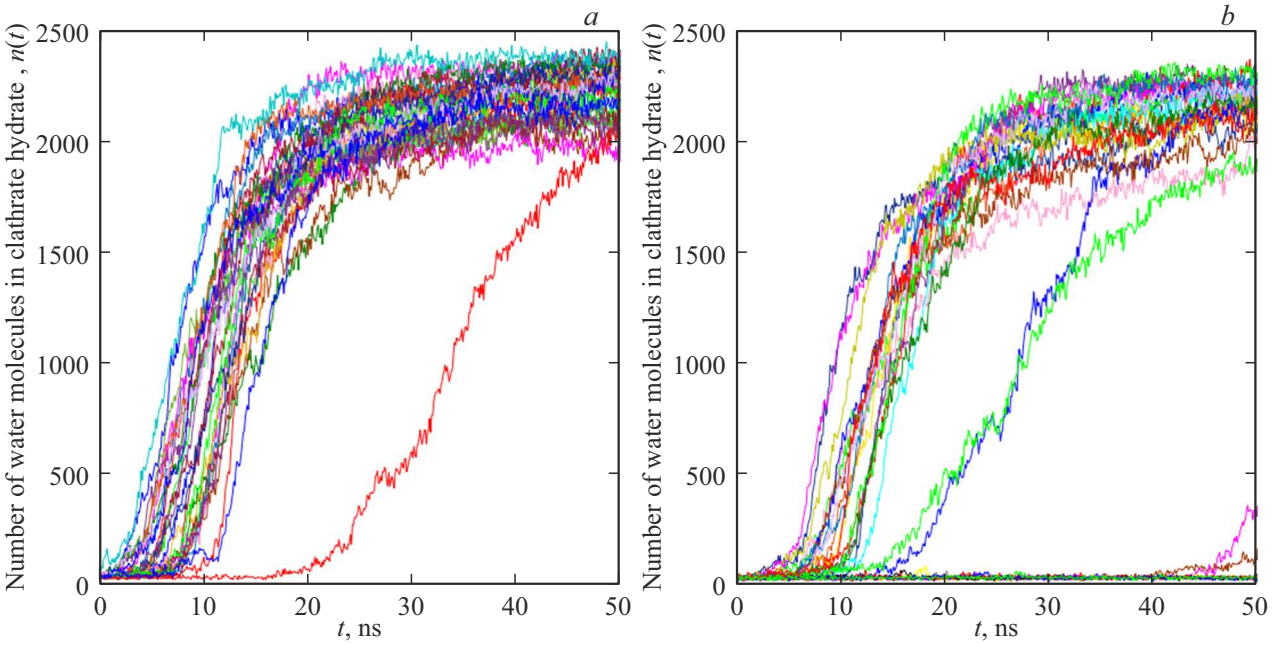

Figure 3. The number of water molecules forming the hydrate structure vs. modelling time at various cooling rates: (a) $\gamma = 1.0$ K/ps and (b) $= 10.0$ K/ps.

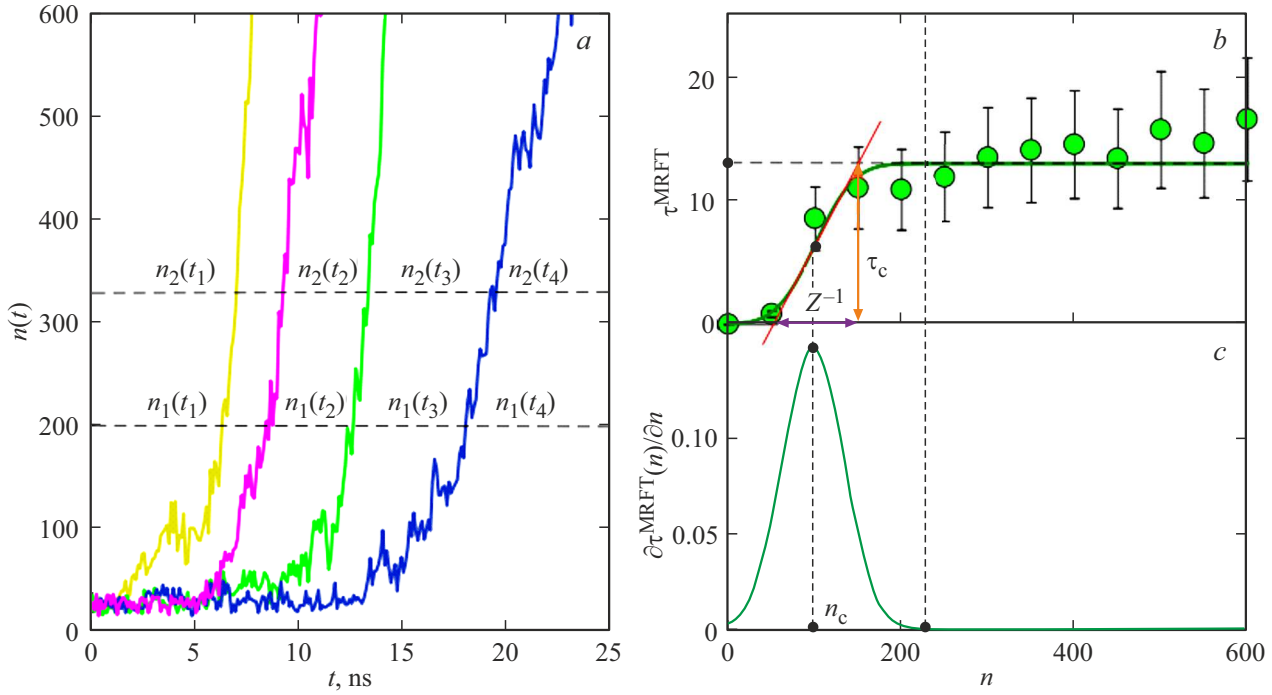

Figure 4. a — schematic views of nucleus growth paths $n(t)$ obtained during four independent numerical experiments. b — MFPT curve plotted by averaged inverted curves $n(t)$. c — the first derivative of MFPT curve: $\partial\tau_l(n)/\partial n$, where the peak defines the critical size $n = n_c$. The estimated average nucleation time scale is $\tau_c = (J \cdot V)^{-1}$.

hydrate nucleation and growth process with different cooling rates ($\gamma = 1.0$ and 10.0 K/ps) for 30 independent molecular dynamics iterations is quantitatively shown as a set of growth paths in Figure 3. Figure shows that, at cooling rate $\gamma = 1.0$ K/ps, gas hydrate nucleation and growth process was observed in all independent molecular dynamics iterations, while no any nucleation event was observed at cooling rate $\gamma = 10.0$ K/ps in eight out of thirty ($\approx 26.7\%$) numerical experiments.

Equation (6) parameters and nucleation process variables

System cooling rate γ, K/ps	Critical nucleus size n_c	Mean nucleation time scale τ_c, *ns*	Zeldovich factor Zeldovich, c	Steady-state nucleation rate J_c, $(\text{Å}^{-3} \cdot \text{ns}^{-1})$	Zeldovich factor, Z
1.0	45 ± 1	6 ± 0.1	0.03	$4.061 \cdot 10^{-5}$	0.0169
10.0	35 ± 2	8 ± 0.12	0.04	$3.045 \cdot 10^{-5}$	0.0226

The nucleation characteristics were further assessed by statistical processing of the largest crystal nucleus growth paths according to independent molecular dynamics calculations — within the mean first passage time method (MFPT) [16]. Thus, for each independent numerical experiment, time dependence of the largest crystalline nucleus size $n_\alpha(t)$, where $\alpha = 1, 2, \ldots, 30$ — is an iteration number. Mean first passage time of a nucleus with size n was determined from a set of paths.

$$\bar{\tau}(n) = \frac{1}{N}\sum_{\alpha=1}^{N} \tau_\alpha(n), \quad \text{where} \quad N = 30. \tag{3}$$

The point of inflection defines critical size n_c and average time τ_c which is necessary to achieve the critical nucleus size.

Figure 4 shows schematic views of MFPT curves plotted on he basis of molecular dynamic calculations. Figure $4, a$ shows nucleus growth paths $n(t)$ plotted by four independent molecular dynamics iterations. For example, for the first largest nucleus, the point of inflection $\tau_1(n)$ (see Figure $4, b$) defines the critical size nc with the mean waiting time $\tau_1 = \tau_1(n_c)$ that corresponds to the peak in derivative $\partial\tau_1(n)/\partial n$ (see Figure $4, c$). Mean nucleation time scale τ_c is defined as a point on the time axis corresponding to the first minimum position on curve $\partial\tau_1(n)/\partial n$.

Steady-state nucleation rate is calculated as

$$J = \frac{1}{\tau_c V}, \tag{4}$$

where V is the system volume. Numerical value for Zeldovich parameter Z may be estimated using the following expression

$$Z = J \cdot V \left.\frac{d\tau_1(n)}{dn}\right|_{n=n_c}, \tag{5}$$

with known J.

Nucleation process parameters were defined by fitting the modelling results for MFPT curves using the following equation [17]:

$$\tau(n) = \frac{\tau_c}{2}\{1 + erf[c(n - n_c)]\}, \tag{6}$$

where c is the scaled Zeldovich factor [18,19] defining the potential barrier curvature in its apex.

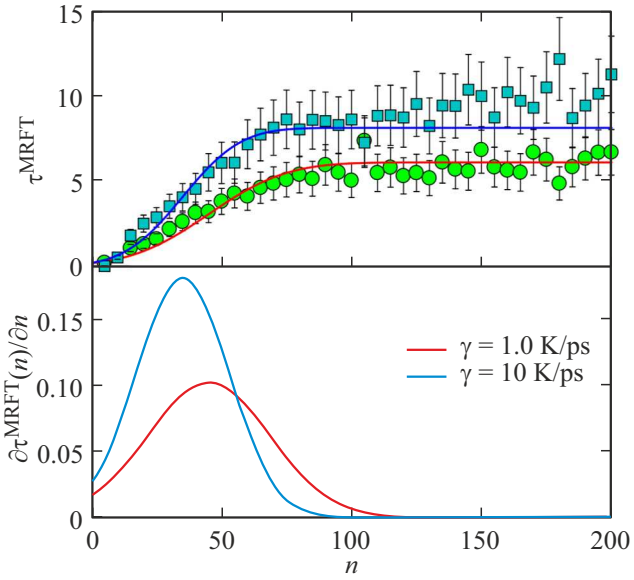

Figure 5. MFPT curve (upper column) and the first derivative (lower column) plots calculated at two system cooling rates: $\gamma = 1.0$ K/ps (circles) and $\gamma = 10.0$ K/ps (squares).

Figure 5 shows MFPT curves obtained from averaged inverted curves $n(t)$ at two various cooling rates $\gamma = 1.0$ and $\gamma = 1.0$ K/ps: markers denote the molecular dynamics modelling results; solid lines are the equation fitting results (6). The figure shows that, with the system cooling rate growth, increase of mean nucleation time scale τ_c and decrease of critical nucleus size n_c are observed (see the lower column). Equation parameters (6) and calculated nucleation process variables are listed in the Table.

4. Conclusion

Molecular dynamics modelling of the hydrate formation process in highly overcooled two-phase „methane–water“ system is described herein. The modelling shows that at rather high cooling rates in the system, crystalline form of methane hydrate still can be formed. It has been shown that homogenous crystalline nucleation scenario is implemented at the initial phase transition stage. It has been found that, with the system cooling rate growth, increase of mean nucleation time scale τ_c and decrease of critical nucleus size n_c are observed.

Funding

This study was supported by the Russian Science Foundation (project No. 22-22-00508). Large-scale molecular dynamics calculations were performed using the equipment of the Center for Collective Use of Ultra-High-performance Computational Resources of Lomonosov Moscow State University and the computation cluster of Kazan (Volga Region) Federal University.

Conflict of interest

The authors declare that they have no conflict of interest.

References

[1] V.K. Michalis, J. Costandy, I.N. Tsimpanogiannis, A.K. Stubos, I.G. Economou. J. Chem. Phys. **142**, 044501 (2015).
[2] N.N. Nguyen, M. Galib, A.V. Nguyen. Energy Fuels **34**, 6751 (2020).
[3] M.B. Yunusov, R.M. Khusnutdinov, A.V. Mokshin. FTT, **63**, 308 (2021). (in Russian).
[4] M.B. Yunusov, R.M. Khusnutdinoff. J. Phys. Conf. Ser. **2270**, 012052 (2022).
[5] M.B. Yunusov, R.M. Khusnutdinov. Uch. zap. fiz. fak-ta Mosk. un-ta **4**, 2240702 (2022).
[6] O. Gaidukova, S. Misyura, P. Strizhak. Energies **15**, 1799 (2022).
[7] A.A. Sizova, V.V. Sizov, E.N. Brodskaya. Kolloid. zhurn. (in Russian). **82**, 223 (2020).
[8] Y.-S. Yu, X. Zhang, J.-W. Liu, Y. Lee, X.-S. Li. Energy Environ. Sci. **14**, 5611 (2021).
[9] A. Abbasi, F.M. Hashim. Petrol. Sci. Tech. **40**, 2382 (2022).
[10] L.C. Jacobson, V. Molinero. J. Phys. Chem. B **114**, 7302 (2010).
[11] S. Plimpton. J. Comput. Phys. **117**, 1 (1995).
[12] L. Verlet. Phys. Rev. **159**, 98 (1967).
[13] A.H. Nguyen, V. Molinero. J. Phys. Chem. B **119**, 9369 (2015).
[14] P.R. ten Wolde, M.J. Ruiz-Montero, D. Frenkel. J. Chem. Phys. **104**, 9932 (1996).
[15] P.J. Steinhardt, D.R. Nelson, M. Ronchetti. Phys. Rev. B **28**, 784 (1983).
[16] A.V. Mokshin, B.N. Galimzyanov. Phys. Chem. Chem. Phys. **19**, 11340 (2017).
[17] J. Wedekind, R. Strey, D. Reguera. J. Chem. Phys. **126**, 134103 (2007).
[18] J.B. Zeldovich. Acta Physicochim. URSS **18**, 1 (1943).
[19] V.G. Baidakov, A.O. Tipeev. FTT **60**, 1803 (2018).

Translated by Ego Translating